Skeleton atomic effect on nonlinear optical properties of linear trinuclear heteroselenometallic compounds with univalent coinage metals

Qian-Feng Zhang,[a,b] Wa-Hung Leung,[b] Ying-Lin Song,[c] Mao-Chun Hong,[d] Colin H. L. Kennard[e] and Xin-Quan Xin*[a]

[a] *Coordination Chemistry Institute and Department of Chemistry, Nanjing University, Nanjing 210093, P. R. China. E-mail: xxin@netra.nju.edu.cn*
[b] *Department of Chemistry, The Hong Kong University of Science and Technology, Clear Water Bay, Kowloon, Hong Kong, P. R. China*
[c] *Department of Physics, Harbin Institute of Technology, Harbin 150001, P. R. China*
[d] *Fujian Institute of Research on Structure of Matter, Chinese Academy of Sciences, Fuzhou, Fujian 350002, P. R. China*
[e] *Department of Chemistry, University of Queensland, Brisbane QLD 4072, Australia*

Received (in Montpellier, France) 18th October 2000, Accepted 11th December 2000
First published as an Advance Article on the web 15th February 2001

Treatment of $[NEt_4]_2[WSe_4]$ with 2 equiv. of $[M(PPh_3)_2(NO_3)]$ (M = Cu or Ag) in CH_2Cl_2 gave the trinuclear cupro- or argento-selenotungstate compounds $[(WSe_4)(MPPh_3)\{M(PPh_3)_2\}]$ (M = Cu **1**, Ag **2**). In compounds **1** and **2**, the $[WSe_4]^{2-}$ anion is bonded to $[M(PPh_3)]^+$ and $[M(PPh_3)_2]^+$ fragments, resulting in trigonal and tetrahedral coordination geometries around M. Treatment of $[NEt_4]_2[WSe_4]$ with $[Au(PPh_3)Cl]$ in a 1 : 2 molar ratio afforded the trinuclear auroselenotungstate compound $[WSe_4(AuPPh_3)_2]$ **3**. For compound **3**, the two equivalent $[Au(PPh_3)]^+$ fragments bind to the $[WSe_4]^{2-}$ symmetrically, and the geometry around the two Au atoms is distorted trigonal planar. Compounds **1–3** are air and optically stable. Their nonlinear optical absorption and refraction along with the optical limiting effects were determined under the same conditions. By comparison of nonlinear optical properties of the three compounds, a skeleton atomic effect on the nonlinear optical properties for heteroselenometallic cluster compounds was outlined. Compound **3** exhibits both large nonlinear optical absorption and refraction (self-focusing). The Ag-containing heteroselenometallic compound **2** may be considered as a good candidate for an optical limiting material.

Tremendous interest has been attracted by nonlinear optical (NLO) processes and materials because of their potential in photonic applications.[1] Much effort has been made in the last two decades in designing new NLO devices and circuits, and in demonstrating their logic operation, signal switch, and energy (power) limiting functions.[2] Great challenges remain in developing superior third-order NLO materials that can utilize short-wavelength laser light sources generated by the newly developed semiconductor diode lasers for optical data processing.[3] In the field of optical limiting (OL), attention has also been drawn to reverse saturable absorption (RSA) in the visible portion of the spectrum. The materials most extensively studied include semiconductors, organic dyes, metallophthalocyanines, and fullerenes.[4,5]

Recently, interesting NLO properties were observed in a variety of inorganic clusters and organometallic compounds. Notable examples of such organometallic NLO materials include the molecular cubane-like clusters $[NBu^n_4][MS_4M'_3BrX_3]$ (M = Mo, W; M′ = Cu, Ag; X = Cl, Br, I), which exhibit strong NLO absorption[6] and King's complex $[(\eta^5\text{-}C_5H_5)Fe(CO)]_4$, which shows excellent optical limiting properties.[7] In our recent efforts to search for new NLO materials, we have investigated the third-order NLO properties of heterometallic sulfur clusters with different structures.[8] For example, strong NLO behavior has been found for the supracage-shaped cluster $[NBu^n_4]_4[Mo_8Cu_{12}O_8S_{24}]$, the twin nest-shaped cluster $[NEt_4]_4[Mo_2Cu_6O_2S_6Br_2I_4]$, and the butterfly-shaped clusters $[MCu_2OS_3(PPh_3)_n]$ (M = Mo, W; $n = 3$, 4).[9] One-dimensional linear chain polymeric clusters $\{[NBu^n_4][MS_4Tl]\}_n$ (M = Mo, W) were found to show large NLO refraction.[10] A very large OL effect has been observed in the hexagonal prism-shaped cluster $[Mo_2Ag_4S_8(PPh_3)_4]$, the cross-frame cluster $[WCu_4S_4(SCN)_2(py)_6]$ (py = pyridine) and the two-dimensional polymeric cluster $\{[WS_4Cu_6I_4(py)_4]\}_n$.[11] Thus, these results suggest that structural alterations in clusters may be responsible for the switching of the NLO properties.

In contrast to the wealth of studies on heterometallic sulfur clusters, there are few studies on the NLO properties of analogous selenide clusters,[12] which may have important applications such as precursors for low-bandgap semiconductors and nonlinear optics.[13] In this context, we set out to extend the studies on NLO properties of heteroselenometallic clusters. One might expect an improvement in the NLO properties of selenium-containing compounds as metal selenium compounds are expected to have higher nonlinear susceptibilities than their sulfur analogs due to the heavy atom effect. In previous studies, we have noticed that skeleton atom substitution in cluster compounds may induce large changes in their NLO properties.[14] To further understand this skeleton atomic effect on the NLO properties, we here report the syntheses, structures and NLO properties of linear tri-

nuclear heteroselenometallic clusters with univalent coinage metals.

Experimental

Measurements and materials

$^{31}P\{^{1}H\}$ NMR spectra were recorded on a Varian Unity-500 spectrometer at 23 °C relative to 85% H_3PO_4. Elemental analyses were carried out on a PE 240C elemental analyzer. Infrared spectra were recorded as KBr pellets on a Nicolet FT-170SX spectrometer. The electronic spectra were measured on a Shimadzu UV-300 spectrophotometer.

Commercially available solid chemicals were of A.R. grade and were used without further purification. Solvents were distilled over appropriate drying agents prior to use. The compounds $[Cu(PPh_3)_2(NO_3)]$ and $[Ag(PPh_3)_2(NO_3)]$ were obtained from reaction of PPh_3 with $Cu(NO_3)_2 \cdot 3H_2O$ and $AgNO_3$, respectively, in CH_3OH–CH_2Cl_2 (2 : 1) solution. The compound [Au(PPh$_3$)Cl] was prepared according to the literature method.[15] $[NEt_4]_2[WSe_4]$ was synthesized by an improvement on the literature procedure.[16] All reactions were performed under a dry nitrogen atmosphere.

Preparations

$[WSe_4(CuPPh_3)\{Cu(PPh_3)_2\}]$ 1. To a solution of $[NEt_4]_2[WSe_4]$ (0.23 g, 0.30 mmol) in MeCN (10 mL) was added a 15 mL CH_2Cl_2 solution of $[Cu(PPh_3)_2(NO_3)]$ (0.40 g, 0.60 mmol). After the reaction mixture had been stirred for 1 h at 25 °C, it was filtered through a medium-porosity sintered glass frit to provide a dark red powder and an orange–red filtrate. Et_2O was slowly diffused into the filtrate, and after 3 days red crystals of **1** were collected. Yield: 0.15 g, 58%. Anal. calc. for $C_{54}H_{45}P_3Se_4Cu_2W$: C, 45.88; H, 3.21%. Found: C, 46.23; H, 3.15%. IR (KBr, cm^{-1}): ν(W–Se), 300(m) and 292(sh). $^{31}P\{^{1}H\}$ NMR ($CDCl_3$): δ 26.73, 28.01.

$[WSe_4(AgPPh_3)\{Ag(PPh_3)_2\}]$ 2. The method was similar to that used for **1**, employing $[Ag(PPh_3)_2(NO_3)]$ (0.43 g, 0.6 mmol) instead of $Cu(PPh_3)_2(NO_3)$. Yield: 0.17 g, 53%. Anal. calc. for $C_{54}H_{45}P_3Se_4Ag_2W$: C, 43.17; H, 3.02%. Found: C, 43.55; H, 3.06%. IR (KBr, cm^{-1}): ν(W–Se), 299(m) and 294(sh). $^{31}P\{^{1}H\}$ NMR ($CDCl_3$): δ 3.74, 3.91.

$[WSe_4(AuPPh_3)_2]$ 3. $[NEt_4]_2[WSe_4]$ (0.23 g, 0.30 mmol) and Au(PPh$_3$)Cl (0.30 g, 0.60 mmol) were dissolved in CH_2Cl_2 (20 mL) to afford a bright orange solution. The reaction mixture was stirred for 45 min at 25 °C and then filtered. The orange filtrate was diffused with Et_2O vapor and orange block crystals of **3** were harvested after 2 days. Yield: 0.21 g, 76%. Anal. calc. for $C_{36}H_{30}P_2Se_4Au_2W$: C, 30.49; H, 2.13%. Found: C, 31.17; H, 2.04%. IR (KBr, cm^{-1}): ν(W–Se), 303(m). $^{31}P\{^{1}H\}$ NMR ($CDCl_3$): δ 52.51.

Crystal structure analyses

The diffraction experiments on $\mathbf{2} \cdot 0.5CH_2Cl_2$ and **3** were carried out on an Enraf–Nonius CAD4 diffractometer, using graphite-monochromated Mo-Kα radiation at room temperature. Intensity profile data were processed and then corrected for absorption effects. The structures were solved by direct methods. All computations were carried out on an IBM/PC-586 computer using the SHELXTL-PC program package.[17] Crystalline **2** contains half a CH_2Cl_2 solvent molecule per molecule of **2**, which is in a general position. The carbon atom is situated at an inversion center and the chlorine atoms are disordered with an occupancy factor of 0.5/0.5. All non-hydrogen atoms except for CH_2Cl_2 were refined anisotropically on F^2. For both structures the positions of the hydrogen atoms were calculated and were included in the final refinements. For those reflections having $F_o^2 > 2\sigma(F_o^2)$ the final cycle of least-squares refinement converged to values of R of 0.0507 (597 variables and 9950 observations for $\mathbf{2} \cdot 0.5CH_2Cl_2$) and 0.0656 (406 variables and 7425 observations for **3**). The largest difference residue peak of 2.766 e Å^{-3} in **3** is near to the gold atoms. Table 1 lists crystallographic and experimental data for $\mathbf{2} \cdot 0.5CH_2Cl_2$ and **3**.

CCDC reference number 440/249. See http://www.rsc.org/suppdata/nj/b0/b008466m/ for crystallographic files in .cif format.

Optical measurements

CH_2Cl_2 solutions (1.2×10^{-3} M) of compounds **1**–**3** were placed in a 1 mm quartz cuvette for NLO measurements. The compounds are stable towards air and laser light. Their nonlinear absorptions and refractions and optical responses were investigated with linearly polarized 7 ns pulses provided by a frequency-doubled, mode-locked, Q-switched Nd : YAG laser. The spatial distribution of the laser ($\lambda = 532$ nm) became nearly Gaussian after passing through a spatial filter. The laser beam was focused with a 25 cm focal length focusing mirror. The radius of the beam circumference was measured to be 30 ± 5 μm (half-width at $1/e^2$ maximum in irradiance). The incident and transmitted pulse energies were measured simultaneously by two energy detectors (Laser Precision RjP-735), which were linked to a computer by an IEEE interface.[18] The NLO properties of the samples were manifested by

Table 1 Crystallographic data for $\mathbf{2} \cdot 0.5CH_2Cl_2$ and **3**

	$\mathbf{2} \cdot 0.5CH_2Cl_2$	**3**
Empirical formula	$C_{54.5}H_{46}P_3ClSe_4Ag_2W$	$C_{36}H_{30}P_2Se_4Au_2W$
Formula weight	1544.69	1418.16
T/K	293	293
Crystal system	Monoclinic	Triclinic
Space group	$P2_1/a$ (no. 14)	$P\bar{1}$ (no. 2)
a/Å	17.921(7)	9.593(2)
b/Å	17.472(3)	10.825(2)
c/Å	18.196(7)	19.936(4)
α/°		89.54(3)
β/°	95.86(2)	80.41(3)
γ/°		68.45(3)
U/Å^3	5667.7(33)	1895.3(7)
Z	4	2
μ(Mo-Kα)/mm^{-1}	5.443	14.699
Reflections collected	9957	7897
Independent reflections	4060	5758
R_{int}	0.0563	0.0288
Final R_1, wR_2 [$I > 2\sigma(I)$]	0.0507, 0.1120	0.0656, 0.1213
[all data]	0.0921, 0.1614	0.0713, 0.1452

moving the samples along the axis of the incident laser irradiance beam (z direction) with respect to the focal point and with incident laser irradiance kept constant (z scan methods). The closed-aperture curves are normalized to the open-aperture curves. An aperture of 0.5 mm radius was placed in front of the detector to measure the transmitted energy when assessment of laser beam distortion was needed. To eliminate scattering effects, a lens was mounted after the samples to collect the scattered light. The solid acceptance angle of the transmitted detector was thus increased by a factor of 1000 from 1.28 to 1.39 rad.

Results and discussion

Synthesis

Synthetic routes to trinuclear heterometallic sulfur clusters starting from $[MS_4]^{2-}$ (M = Mo or W) were found to be applicable for the metal selenium cluster analog.[19] Thus, when $[Cu(PPh_3)_2]^+$ and $[Ag(PPh_3)_2]^+$ reacted with $[WSe_4]^{2-}$ anion in the absence of halide anions, the corresponding PPh_3-ligated trimetallic cupro- and argento-selenotungstates $[(WSe_4)(M'PPh_3)\{M(PPh_3)_2\}]$ (M = Cu **1** and Ag **2**) were produced. For compounds **1** and **2**, a $[M(PPh_3)]^+$ fragment binds to two Se of the $[WSe_4]^{2-}$ while the remaining two Se bind to a $[M(PPh_3)_2]^+$ fragment. The geometries around the three and four-coordinate M are distorted trigonal planar and tetrahedral, respectively [Scheme 1(a)]. If halides were present in the reaction mixture, the tetranuclear cubane-like clusters $[(WSe_4)(MPPh_3)_3X]$ (X = Cl, Br and I) were isolated [Scheme 1(b)]. However, reaction of $[Au(PPh_3)]^+$ with $[WSe_4]^{2-}$ only afforded the trimetallic auroselenotungstate compound $[WSe_4(AuPPh_3)_2]$ (**3**), in which the $[WSe_4]^{2-}$ anion binds two $[Au(PPh_3)]^+$ fragments symmetrically [Scheme 1(c)]. The reaction was found to be unaffected by the presence of halide anions.

It appears that the stoichiometry of the coinage metal heteroselenometalate cluster formed is not affected by the $[WSe_4]^{2-}$: $[M(PPh_3)_n]^+$ ratio, but is dependent on the nature of the univalent fragments $[M(PPh_3)_n]^+$ (M = Cu, Ag; n = 1–3). For example, the same cluster compounds were obtained even when $[WSe_4]^{2-}$ was treated with 3 equiv. of $[M(PPh_3)_2]^+$. It may be noted that Müller and coworkers reported the isolation of an argentoselenotungstate compound $[WSe_4(AgPPh_3)_2]$ by the reaction of $[Ag(PPh_3)]^+$ with $[WSe_4]^{2-}$ although no structural characterization was made.[20] The Mo(W)/Cu(Ag,Au)/S and Mo/Au/Se analogs for heterometallic compounds **1**–**3** are known.[19,21] Related coinage metal heteroselenometalates $[WSe_4\{M(PMe_2Ph)_2\}_2]$ (M = Cu, Ag, Au), $[WSe_4(AuPMe_2Ph)_2]$, $[Ph_4P]_2[WSe_4\{M(CN)\}_2]$ (M = Cu, Au) and $[Ph_4P]_2[MoSe_4\{M(CN)\}_2]$ (M = Cu, Au) have also been previously reported by Ibers and coworkers.[22]

Crystal structures

The structure of $\mathbf{2}\cdot 0.5CH_2Cl_2$ was confirmed by an X-ray diffraction study. The molecular structure of **2** is shown in Fig. 1

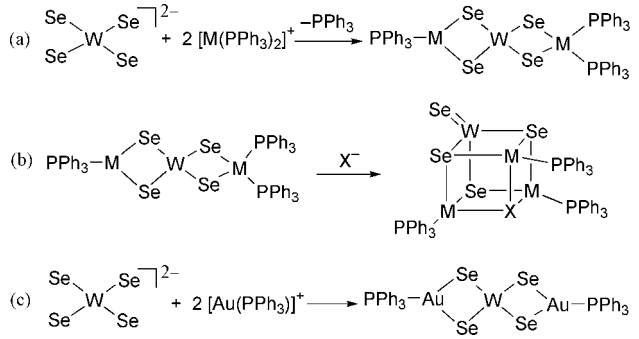

Scheme 1

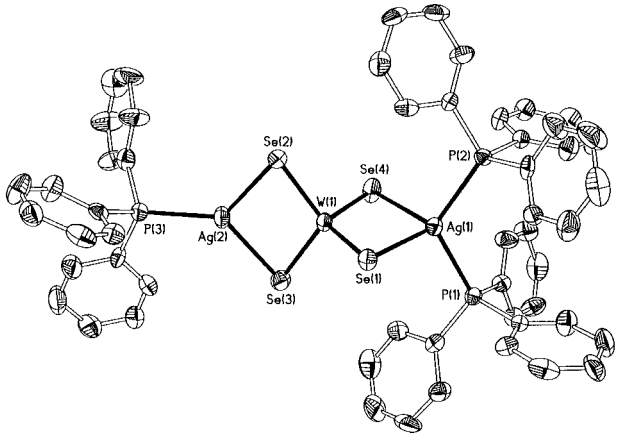

Fig. 1 Crystal structure of $[WSe_4(AgPPh_3)\{Ag(PPh_3)_2\}]$ **2**.

and selected bond lengths and angles are given in Table 2. The tungsten atom has an essentially tetrahedral coordination geometry with W–Se distances ranging from 2.320(2) to 2.345(2) Å, which are longer than those in free $[WSe_4]^{2-}$ as expected. There are two different types of silver atoms in **2**: one has tetrahedral geometry, being bonded to two phosphorus and two selenium atoms; whereas the other has a trigonal planar geometry, being bonded to one phosphorus and two selenium atoms. The W···Ag distance for the 3-coordinate silver of 2.9120(12) Å is slightly shorter than that for the 4-coordinate counterpart [3.0797(12) Å]. The average W···Ag separation in $\mathbf{2}\cdot 0.5CH_2Cl_2$ [2.9958(12) Å] is comparable to those in other W/Ag/Se cluster compounds such as $[WAg_2Se_4(C_5H_5NS)(PPh_3)_2]\cdot CH_2Cl_2$ [3.014(2) Å] and $[WAg_3Se_4(PPhMe_2)_3I]$ [2.976(1) Å][23] and is significantly longer than the W···Au distances in **3**.

Fig. 2 shows the structure of **3** and Table 3 lists selected bond lengths and angles. Compound **3** is isostructural to the sulfur analogs $[MS_4(AuRPh_3)_2]$ (M = Mo, W; R = P, As)[19] and heteroselenometallic compounds $[MoSe_4(AuPPh_3)_2]$ and

Table 2 Selected bond lengths (Å) and angles (°) for $\mathbf{2}\cdot 0.5CH_2Cl_2$

W(1)–Se(1)	2.325(2)	W(1)–Se(2)	2.345(2)
W(1)–Se(3)	2.337(2)	W(1)–Se(4)	2.320(2)
Ag(1)–Se(1)	2.644(2)	Ag(2)–Se(2)	2.543(2)
Ag(2)–Se(3)	2.547(2)	Ag(1)–Se(4)	2.646(2)
Ag(1)–P(1)	2.462(4)	Ag(1)–P(2)	2.468(4)
Ag(2)–P(3)	2.385(4)		
W(1)···Ag(1)	3.0797(12)	W(1)···Ag(2)	2.9120(12)
Se(4)–W(1)–Se(1)	113.12(5)	Se(4)–W(1)–Se(3)	108.15(8)
Se(1)–W(1)–Se(3)	106.99(7)	Se(4)–W(1)–Se(2)	107.30(7)
Se(1)–W(1)–Se(2)	108.05(7)	Se(3)–W(1)–Se(2)	113.36(6)
Se(1)–Ag(1)–Se(4)	94.23(5)	Se(2)–Ag(2)–Se(3)	100.45(6)
W(1)–Se(1)–Ag(1)	76.31(5)	W(1)–Se(2)–Ag(2)	73.01(6)
W(1)–Se(3)–Ag(2)	73.07(6)	W(1)–Se(4)–Ag(1)	76.34(6)
P(1)–Ag(1)–P(2)	120.15(13)	P(1)–Ag(1)–Se(1)	106.83(11)
P(2)–Ag(1)–Se(1)	115.32(11)	P(1)–Ag(1)–Se(4)	112.63(12)
P(2)–Ag(1)–Se(4)	104.71(11)	P(3)–Ag(2)–Se(2)	129.64(12)
P(3)–Ag(2)–Se(3)	129.91(12)	C(18)–P(1)–Ag(1)	115.8(5)

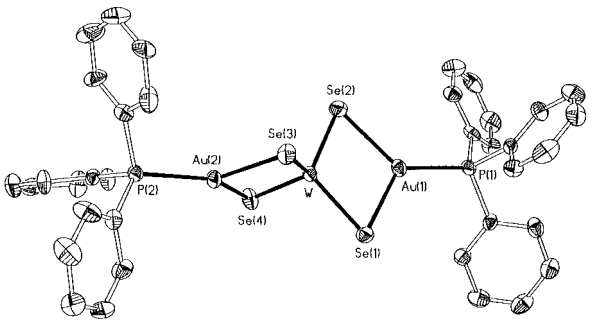

Fig. 2 Crystal structure of $[WSe_4(AuPPh_3)_2]$ **3**.

Table 3 Selected bond lengths (Å) and angles (°) for **3**

W–Se(1)	2.362(2)	W–Se(2)	2.354(2)
W–Se(3)	2.356(2)	W–Se(4)	2.353(2)
Au(1)–Se(1)	2.518(2)	Au(1)–Se(2)	2.509(2)
Au(2)–Se(3)	2.529(2)	Au(2)–Se(4)	2.518(2)
Au(1)–P(1)	2.292(4)	Au(2)–P(2)	2.299(4)
W···Au(1)	2.8642(12)	W···Au(2)	2.8893(13)
Se(4)–W–Se(2)	107.45(8)	Se(4)–W–Se(3)	112.81(7)
Se(2)–W–Se(3)	108.29(8)	Se(4)–W–Se(1)	107.42(8)
Se(2)–W–Se(1)	113.06(7)	Se(3)–W–Se(1)	107.92(7)
Se(2)–Au(1)–Se(1)	102.98(6)	Se(4)–Au(2)–Se(3)	102.03(6)
W–Se(1)–Au(1)	71.79(5)	W–Se(2)–Au(1)	72.09(6)
W–Se(3)–Au(2)	72.42(6)	W–Se(4)–Au(2)	72.67(6)
P(1)–Au(1)–Se(2)	132.40(12)	P(1)–Au(1)–Se(1)	124.46(12)
P(2)–Au(2)–Se(4)	134.18(12)	P(2)–Au(2)–Se(3)	123.52(11)

$[WSe_4(AuPPhMe_2)_2]$.[21,22] The geometry around W in **3** is slightly distorted tetrahedral. The deviation from tetrahedral geometry around W is more pronounced than that in the sulfur analog. The geometry around Au is distorted trigonal planar with Se–Au–Se angles of 102.98(6) and 102.03(6)°. The three metal atoms and two phosphorus atoms are approximately collinear, with the Au···W···Au and two P–Au···W angles deviating less than 8° from 180°. The Au–Se bond lengths are, of course, longer than the corresponding Au–S distances because of the bigger covalent radius of selenium compared with that of sulfur.[19] The Au–P distances in **3** [av. 2.295(2) Å], however, are shorter than the Ag–P distance in $\mathbf{2}\cdot 0.5CH_2Cl_2$ [2.385(4) Å], suggesting that the Au–P bond is stronger than the Ag–P bond. Similarly, it may be deduced that the formal $W^{VI}\cdots Au^{I}$ interactions are stronger than the $W^{VI}\cdots Ag^{I}$ interactions because the W···Au distances in **3** are shorter than the W···Ag distances in $\mathbf{2}\cdot 0.5CH_2Cl_2$. The average W···Au and Au–Se distances in **3** agree well with those in other auroselenometalllic compounds.[22]

Spectroscopic properties

The IR spectra of compounds **1**–**3** display typical absorption peaks at about 1478, 1435, 998, 740, 692 and 530 cm^{-1}, which are characteristic for the PPh_3 ligand. The metal–phosphorous stretches appear as medium bands in the range 340–420 cm^{-1}. The W–Se stretching vibrations for **1**, **2** and **3** were found in the region of 290–303 cm^{-1}, which are slightly red-shifted compared to that of free $[WSe_4]^{2-}$ (305 cm^{-1}).[24]

The $^{31}P\{^1H\}$ NMR spectra of **1** and **2** show two singlets, suggesting that there are two chemically inequivalent phosphorus atoms in these compounds. On the other hand, compound **3** only shows a single ^{31}P signal due to the magnetically equivalent phosphorus nuclei. The ^{31}P chemical shifts for compounds **1** and **2** are further downfield than that for **3**, probably because of good orbital overlap between P and Au^+, which has a bigger covalent radius than Ag^+. Despite the larger ionic radius of Ag(I) compared with Cu(I), the ^{31}P signal for **2** was found to be further downfield than that for **1**. This may be because the longer Ag–P and Ag–Se bond distances decrease the ^{31}P deshielding effect. Our results, together with the previously reported ^{31}P NMR data for related compounds,[21] suggest that the ^{31}P chemical shifts for argentoselenometallic phosphine compounds are not very sensitive to coordination environments of the metals. No ^{31}P–^{107}Ag coupling is observed in **2**, probably because of phosphorus exchange.

Fig. 3 shows the electronic absorption spectra of compounds **1**, **2** and **3**. The absorption bands at 456, 431 and 420 nm are attributed to the π(Se) → d(W) charge-transfer (CT) transition in the WSe_4 moiety.[22] These bands for the cluster compounds were found to be blue-shifted relative to that for $[WSe_4]^{2-}$. Thus, it appears that the Se → W CT transition energy is significantly affected by the coordination of coinage-metal complex species to $[WSe_4]^{2-}$, indicative of strong interactions between the coinage metal and the $[WSe_4]^{2-}$ moiety.[25]

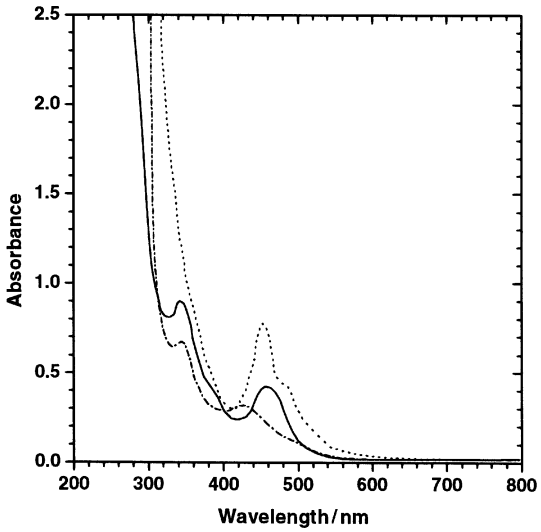

Fig. 3 Electronic absorption (UV-vis) spectra of **1** (——), **2** (– – –) and **3** (–·–·), all at 1.2×10^{-3} M in CH_2Cl_2. The optical path is 1 mm.

NLO absorption and refraction

The nonlinear optical properties of compounds **1**–**3** were investigated using the *z*-scan technique. The *z*-scan results without and with the aperture are given in Fig. 4 and 5, respectively. Fig. 4 clearly illustrates that the absorption increases as the incident light irradiance rises, which is characteristic of a reverse saturable absorption (RSA) process. The non-linear effects in the present cluster compounds are caused by electronic rather than thermal factors. Based on the previous time-resolved nonlinear transmission studies,[26] we found that the nonlinear absorption decreases as the pulse time range elongates. The origin of the observed RSA in compounds **1**–**3** can be attributed to excited-state absorption. Fig. 5 indicates that there are different signs of refractive nonlinearity among compounds **1**–**3**. To obtain the NLO parameters, we employed a *z*-scan theory[18] that considers an effective nonlinearity of third-order nature. Both the absorp-

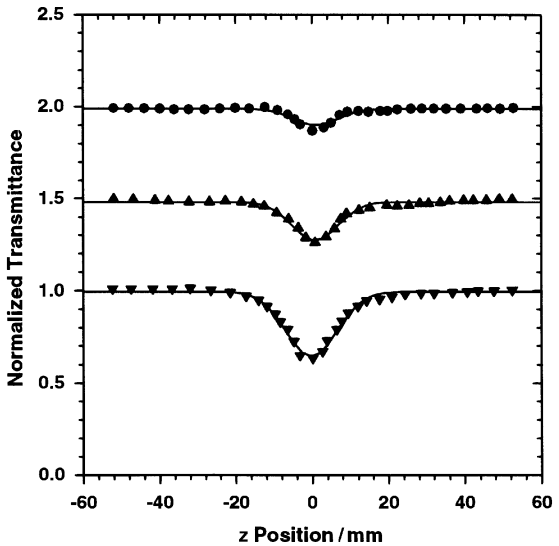

Fig. 4 Open-aperture *z*-scan data of compounds **1** (●), **2** (▲) and **3** (▼) in CH_2Cl_2 solution at 532 nm with incident irradiance $I_i(0) = 110$ MW cm^{-2} and 7 ns laser pulses. Optical path: 1 mm. The solid curves are theoretical fits based on *z*-scan theoretical calculations. The *z*-scan results of **1** and **2** have been shifted vertically by 1.0 and 0.5, respectively, for clarity.

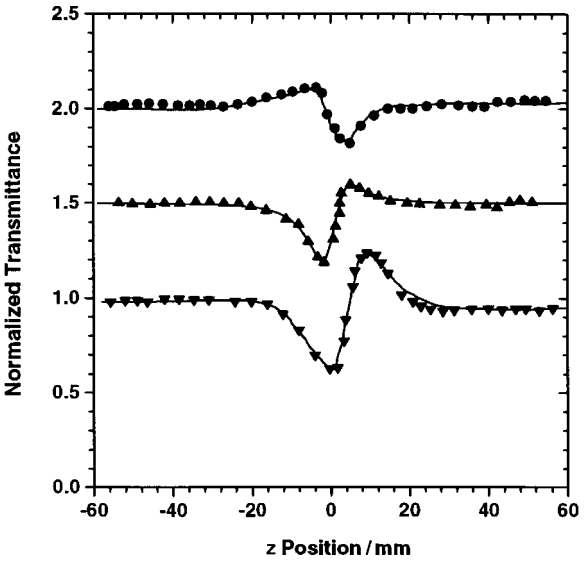

Fig. 5 Closed-aperture *z*-scan data of compounds **1** (●), **2** (▲) and **3** (▼) in CH_2Cl_2 solution measured with a 2.5 cm diameter aperture at incident irradiance $I_i(0) = 110$ MW cm^{-2}. Optical path: 1 mm. The solid curves are theoretical fits based on *z*-scan theoretical calculations. The *z*-scan results of **1** and **2** have been shifted vertically by 1.0 and 0.5, respectively, for clarity.

tion coefficient and refractive index can be expressed as $\alpha = \alpha_0 + \alpha_2 I$ and $n = n_0 + n_2 I$, respectively, where α_0 and α_2 are the linear and nonlinear absorption coefficients; n_0 and n_2 are the linear and nonlinear refractive indices, respectively; and I is the irradiance of the laser beam within the sample. By applying the *z*-scan theory, the solid curves in Fig. 4 and 5 are numerically calculated to fit to the experimental data. The best fits were for $\alpha_2 = 2.1 \times 10^{-6}$ cm W^{-1} M^{-1} and $n_2 = -5.2 \times 10^{-10}$ cm^2 W^{-1} M^{-1} for compound **1**, $\alpha_2 = 8.4 \times 10^{-5}$ cm W^{-1} M^{-1} and $n_2 = 8.7 \times 10^{-10}$ cm^2 W^{-1} M^{-1} for compound **2**, and $\alpha_2 = 1.2 \times 10^{-4}$ cm W^{-1} M^{-1} and $n_2 = 2.3 \times 10^{-9}$ cm^2 W^{-1} M^{-1} for compound **3**.

From the above nonlinear absorptive and refractive data, an evident skeletal atom effect on the nonlinear optical properties was observed. For compounds **1**, **2** and **3** a significant improvement of the NLO absorption was observed upon going from cuproselenotungstate **1** to auroselenotungstate **3** as the size of coinage metal increases, indicative of a heavy atom effect. It should be noted that such a heavy atom effect on the efficiency of nonlinear absorption has also been observed for metallophthalocyanine systems.[27] Thus, firstly, for selenometallic clusters of similar structure, when the copper atom is replaced with the heavier silver atom, the spin–orbital coupling and ionization/geminate recombination become more efficient and thus result in more efficient usage of the triplet excited-state absorption. Second, regardless of a minor influence of the peripheral ligands with similar properties, gold-containing compounds were found to have a relatively large NLO effect. A large third-order molecular susceptibility was measured in the transparent region for $[WS_4Au_2(AsPh_3)_2]$.[28] The present auroselenotungstate compound **3** also exhibits both large nonlinear absorption and large refraction. From Fig. 4 we see that gold-containing compounds should have wider optical transparent windows as compared with the corresponding copper- and silver-containing compounds. Third, the n_2 data of compounds **1**–**3** give an indication of nonlinear refraction: a negative sign for the refractive nonlinearity of **1** gives rises to self-defocusing, while **2** and **3** with a positive sign for the refractive nonlinearity have self-focusing properties. Even if compounds **1** and **2** have a similar structure, their NLO refraction properties are obviously different. The refractive nonlinearity seems to be highly sensitive to the nature of the skeletal atoms. Similar phenomena were found for other isostructural compounds, for example, $[MoOS_3Cu_3I(py)_5]$ and $[WOS_3Cu_3I(py)_5]$, which show self-defocusing and self-focusing properties, respectively;[29] $[MoS_4Au_2(AsPh_3)_2]$ and $[WS_4Au_2(AsPh_3)_2]$ also exhibit self-defocusing and self-focusing properties, respectively.[28] Because only a few examples are found in the literature for comparison, we cannot conclude definitively that the heavy metal atom effect is responsible for the switching of refractive nonlinearity from self-defocusing to self-focusing. Nevertheless the skeletal atomic effect, as well as the influence of structural variation, on the NLO refraction of metal-chalcogenide clusters is apparent.

Optical limiting effect

The optical limiting effects of compounds **1**–**3** were also investigated. Fig. 6 shows the 7 ns optical limiting experimental results of the samples in CH_2Cl_2 solutions at the same concentration (1.2×10^{-3} M). The linear transmittance at 532 nm is 69% and the dynamic range for these optical limiters range from 0.5 to 2.0 J cm^{-2} (fluence). The transmittances of the samples were found to decrease as the laser fluence increases, characteristic of optical limiting.[30] The limiting threshold was defined as the incident fluence at which the transmittance falls to 50% of the linear transmittance. From Fig. 6, the limiting thresholds of compounds **1**, **2** and **3** were determined to be *ca.* 3.0, 1.4 and 1.3 J cm^{-2}, respectively. The saturation fluence transmitted is *ca.* 5 J cm^{-2}. It should be pointed out that our measurements of the transmitted pulse energy were conducted with the aperture placed in front of the transmission detector. Therefore, the observed optical limiting behavior for the compounds can be attributed to both nonlinear absorptive and refractive processes.

Comparing the optical limiting (OL) capabilities of the three compounds, a higher limiting threshold for cuproselenotungstate **1** may be expected due to its low NLO absorption and refraction. However, the optical limiting threshold of argentoselenotungstate **2** is very close to that of auroselenotungstate cluster **3**, although the NLO effect of **3** is much higher than that of **2**. It is not clear whether the nonlinear refraction for these compounds is directly related to the optical limiting effect. As a matter of fact, the optical limiting effect of most Ag-containing clusters at a similar wavelength and with similar linear transmittance was found to be better than in the corresponding Cu-containing counterparts.[14,31] Compared with the Au-containing compound **3**, the better optical limiting effect in the Ag-containing compound **2** may be explained in terms of the corresponding longer bond parameters in **2**, which results in a larger ratio of excited state

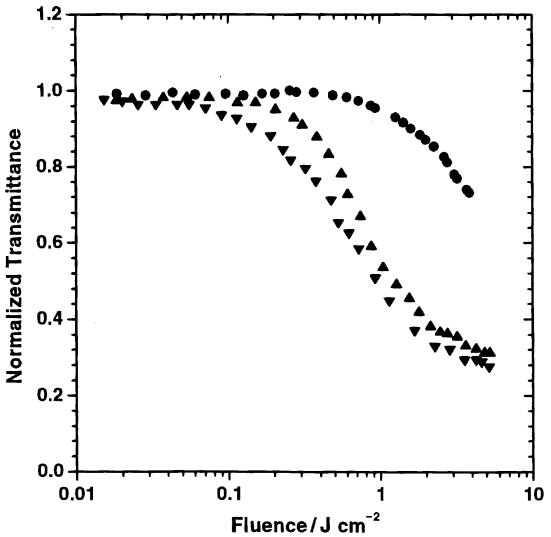

Fig. 6 The 7 ns optical limiting effect of compounds **1** (●), **2** (▲) and **3** (▼), all at 1.2×10^{-3} M in CH_2Cl_2 solution. The energy transmittance is plotted *vs.* the incident fluence.

to ground state absorption (σ_e/σ_g). Based on previous theoretical calculations, the optical limiting capability originates from excited state absorption. Thus, the larger the value of σ_e/σ_g is, the better the optical limiting performance.[32] The values of σ_e and σ_g are *ca.* 4.52 and 2.31 eV, respectively. More proof is, however, required to further verify this theory. In addition, support for the good optical stability of these three compounds arises from the finding that the samples remained effective and chemically intact (no change was found in the ^{31}P NMR signal) in solution during the optical limiting measurements.

Conclusions

In summary, three linear trinuclear cluster compounds with univalent coinage metals and tetraselenotungstate were synthesized and fully characterized. Their nonlinear optical properties have been investigated. The NLO absorption and refraction data along with the optical limiting effect of the three compounds were determined under similar conditions. The difference in NLO properties for these metal cluster compounds are attributed to the influence of the skeleton atoms. It is apparent that the NLO absorptive and refractive properties for linear metal clusters as well as cubane-like clusters are highly sensitive to the heavy atom effect. The auroselenotungstate compound $[WSe_4(AuPPh_3)_2]$ shows both large NLO absorption and large NLO refraction. By comparison with results of the optical limiting effects, the argentoselenotungstate cluster appears to be the best candidate for an optical limiting material among the heteroselenometallic compounds studied thus far.

Acknowledgements

We thank the Ministry of Education of China and the Hong Kong University of Science and Technology for support. We are also grateful for the referees' helpful comments and suggestions for revising the manuscript.

References

1 *Materials for Nonlinear Optics, Chemical Perspectives*, ed. S. R. Marder, J. E. Sohn and G. D. Stucky, American Chemical Society, Washington, DC, 1991; *Nonlinear Optics of Organic Molecules and Polymers*, ed. H. S. Nalwa and S. Miyata, CRC Press, Boca Raton, FL, 1997.
2 M. J. Soileau, W. E. Williams and E. W. Van Stryland, *IEEE J. Quantum Electron.*, 1983, **QE-19**, 731; S. K. Han, Z. Huo, R. Srivastava and R. V. Ramaswamy, *J. Opt. Soc. Am.*, 1989, **6**, 663; D. J. Hagan, T. Xia, A. A. Said, T. H. Wei and E. W. Van Stryland, *Int. J. Nonlinear Opt. Phys.*, 1993, **2**, 483.
3 J. L. Bredas, C. Adant, P. Tackx and A. Persoons, *Chem. Rev.*, 1994, **94**, 243; H. Nakanishi, *Nonlinear Opt.*, 1991, **1**, 223; M. A. Haase, J. Qiu, J. M. Depuydt and H. Cheng, *Appl. Phys. Lett.*, 1991, **59**, 1272.
4 E. W. Van Stryland, Y. Y. Wu, D. J. Hagan, M. J. Soileau and K. Mansour, *J. Opt. Soc. Am.*, 1988, **5**, 1980; G. R. Giuliano and L. D. Hess, *IEEE J. Quantum Electron.*, 1967, **3**, 358; J. S. Shirk, R. G. S. Pong, F. T. Bartoli and A. W. Snow, *Appl. Phys. Lett.*, 1993, **63**, 1880; J. M. Perry, K. Mansour, I. Y. S. Lee, X. L. Wu, P. V. Bedworth, C. T. Chen, D. Ng, S. R. Marder, P. Miles, T. Wada, M. Tian and H. Sasabe, *Science*, 1996, **273**, 1533.
5 L. W. Tutt and A. Kost, *Nature* (*London*), 1992, **19**, 225; D. G. Mclean, R. L. Sutherland, M. C. Brant, D. M. Brandelik, P. A. Fleity and T. Pottenger, *Opt. Lett.*, 1993, **18**, 858.
6 S. Shi, W. Ji, S. H. Tang, J. P. Lang and X. Q. Xin, *J. Am. Chem. Soc.*, 1994, **116**, 3615; S. Shi, W. Ji, J. P. Lang and X. Q. Xin, *J. Phys. Chem.*, 1994, **98**, 3570.
7 T. F. Boggess, G. R. Allan, S. J. Rychnovsky, D. R. Labergerie, C. H. Venzke, A. L. Smirl, L. W. Tutt, A. R. Kost, S. W. McCahon and M. B. Klein, *Opt. Eng.*, 1993, **32**, 1063; G. R. Allan, D. R. Labergerie, S. J. Rychnovsky, T. F. Boggess, A. L. Smirl and L. W. Tutt, *J. Phys. Chem.*, 1992, **96**, 6313.
8 H. W. Hou, X. Q. Xin and S. Shi, *Coord. Chem. Rev.*, 1996, **153**, 25.
9 S. Shi, W. Ji and X. Q. Xin, *J. Phys. Chem.*, 1995, **99**, 894; H. W. Hou, X. Q. Xin, J. Liu, M. Q. Chen and S. Shi, *J. Chem. Soc., Dalton Trans.*, 1994, 3211; S. Shi, W. Ji, W. Xie, T. C. Chong, H. C. Zeng, J. P. Lang and X. Q. Xin, *Mater. Chem. Phys.*, 1995, **39**, 298.
10 J. P. Lang, K. Tatsumi, H. Kawaguchi, J. M. Lu, P. Ge, W. Ji and S. Shi, *Inorg. Chem.*, 1996, **35**, 7924.
11 W. Ji, S. Shi, H. J. Du, P. Ge, S. H. Tang and X. Q. Xin, *J. Phys. Chem.*, 1995, **99**, 17297; M. K. M. Low, H. W. Hou, H. G. Zheng, W.-T. Wong, G. X. Jin, X. Q. Xin and W. Ji, *Chem. Commun.*, 1998, 505; H. W. Hou, Y. T. Fan, C. X. Du, Y. Zhu, W. L. Wang, X. Q. Xin, M. K. M. Low, W. Ji and H. G. Ang, *Chem. Commun.*, 1999, 647.
12 M. A. Ansari and J. A. Ibers, *Coord. Chem. Rev.*, 1990, **100**, 223; L. C. Roof and J. W. Kolis, *Chem. Rev.*, 1993, **93**, 1037.
13 See any issue of *The Bulletin of the Selenium-Tellurium Development Association*, Grimbergen, Belgium, 1991.
14 S. Shi, H. W. Hou and X. Q. Xin, *J. Phys. Chem.*, 1995, **99**, 4050; D. L. Long, S. Shi, X. Q. Xin, B. S. Lou, L. R. Chen, X. Y. Huang and B. S. Kang, *J. Chem. Soc., Dalton Trans.*, 1996, 2617.
15 R. Usón and A. Laguna, *Inorg. Synth.*, 1982, **21**, 71.
16 S. C. O'Neal and J. W. Kolis, *J. Am. Chem. Soc.*, 1988, **110**, 1971.
17 G. M. Sheldrick, *SHELXTL-97, ver. 5.1, Software Reference Manual*, Bruker AXS, Inc., Madison, WI, USA, 1997.
18 M. Sheik-Bahae, A. A. Said and E. W. Van Stryland, *Opt. Lett.*, 1989, **14**, 955; M. Sheik-Bahae, A. A. Said, T. H. Wei, D. J. Hagan and E. W. Van Stryland, *IEEE J. Quantum. Electron.*, 1990, **26**, 760.
19 A. Müller, H. Bögge and U. Schimanski, *Inorg. Chim. Acta*, 1983, **69**, 5; J. M. Charnock, S. Bristow, J. R. Nicholson and C. D. Garner, *J. Chem. Soc., Dalton Trans.*, 1987, 303; F. Canales, M. C. Gimeno, P. G. Jones and A. Laguna, *J. Chem. Soc., Dalton Trans.*, 1997, 439.
20 A. Müller, U. Wienböker and M. Penk, *Chimia*, 1989, **43**, 50.
21 Q. F. Zhang, R. Cao, M. C. Hong, D. X. Wu, W. J. Zhang, Y. Zheng and H. Q. Liu, *Inorg. Chim. Acta*, 1998, **271**, 93.
22 C. C. Christuk, M. A. Ansari and J. A. Ibers, *Inorg. Chem.*, 1992, **31**, 4365; R. J. Salm and J. A. Ibers, *Inorg. Chem.*, 1994, **33**, 4216; R. J. Salm, A. Misetic and J. A. Ibers, *Inorg. Chim. Acta*, 1995, **240**, 239.
23 Q. M. Wang, X. T. Wu, Q. Huang, T. L. Sheng and P. Lin, *Polyhedron*, 1997, **16**, 1439; M. A. Ansari, J. C. Bollinger, C. C. Christuk and J. A. Ibers, *Acta Crystallogr., Sect. C*, 1994, **50**, 869.
24 A. Müller, E. Diemann, R. Josters and H. Bögge, *Angew. Chem., Int. Ed. Engl.*, 1981, **20**, 934.
25 M. A. Ansari, C.-N. Chau, C. H. Mahler and J. A. Ibers, *Inorg. Chem.*, 1989, **28**, 650.
26 W. Ji, W. Xie, S. H. Tang and S. Shi, *Mater. Chem. Phys.*, 1996, **43**, 45; H. W. Hou, B. Liang, X. Q. Xin, K. B. Yu, P. Ge, W. Ji and S. Shi, *J. Chem. Soc., Faraday Trans.*, 1996, **92**, 2343.
27 T. H. Wei, D. J. Hagan, M. J. Sence, E. W. Van Stryland, J. W. Perry and D. R. Coulter, *Appl. Phys. B*, 1992, **54**, 46; A. Dogariu, T. Xia, D. J. Hagan, A. A. Said, E. W. Van Stryland and N. Bloembergen, *J. Opt. Soc. Am. B*, 1996, **14**, 796.
28 H. G. Zheng, W. Ji, M. L. K. Low, G. Sakane, T. Shibahara and X. Q. Xin, *J. Chem. Soc., Dalton Trans.*, 1997, 2357.
29 P. Ge, S. H. Tang, W. Ji, S. Shi, H. W. Hou, D. L. Long, X. Q. Xin, S. F. Lu and Q. J. Wu, *J. Phys. Chem. B*, 1997, **101**, 27.
30 W. Ji, H. J. Du, S. H. Tang and S. Shi, *J. Opt. Soc. Am. B*, 1995, **12**, 876; T. Xia, A. Dogariu, K. Mansour, D. J. Hagan, A. A. Said and E. W. Van Stryland, *J. Opt. Soc. Am. B*, 1998, **15**, 1497.
31 Q. F. Zhang, Y. N. Xiong, T.-S. Lai, W. Ji and X. Q. Xin, *J. Phys. Chem. B*, 2000, **104**, 3476.
32 S. Shi, Z. Lin, Y. Mo and X. Q. Xin, *J. Phys. Chem.*, 1996, **100**, 10696.